Aqueous synthesis of technetium doped titanium dioxide by direct oxidation of titanium powder, a precursor for ceramic nuclear waste forms

Wayne W. Lukens[1]*, Sarah A. Saslow[2]

1) Chemical Sciences Division, Lawrence Berkeley National Laboratory, Berkeley, CA 94720

2) Geosciences Division, Pacific Northwest National Laboratory, Richland, WA 99354

* MS 70A-1150, Lawrence Berkeley National Laboratory, Berkeley, CA 94720. Phone (510) 486-4305; Fax (510) 486-5596. WWLukens@lbl.gov.

Abstract

Technetium-99 (Tc) is a problematic fission product that complicates the long-term disposal of nuclear waste due to its long half-life, high fission yield, and the environmental mobility of pertechnetate, its stable form in aerobic environments. One approach to preventing Tc contamination is through incorporation into durable waste forms based on weathering-resistant minerals such as rutile (titanium dioxide). Here, the incorporation of technetium into titanium dioxide by means of simple, aqueous chemistry – direct oxidation of titanium powder in the presence of ammonium fluoride – is achieved. X-ray absorption fine structure spectroscopy and diffuse reflectance spectroscopy indicate that Tc(IV) replaces Ti(IV) within the structure. Rather than being incorporated as isolated Tc(IV) ions, Tc is present as pairs of edge-sharing Tc(IV) octahedra similar to molecular Tc(IV) complexes such as $[(H_2EDTA)Tc^{IV}](\mu\text{–}O)_2$. Technetium-

doped TiO_2 was suspended in deionized water under aerobic conditions, and the Tc leached under these conditions was followed for 8 months. The normalized release rate of Tc (LR_{Tc}) from the TiO_2 particles is low (3×10^{-6} g m^{-2} d^{-1}), which illustrates the potential utility of TiO_2 as waste form. However, the small size of the as-prepared TiO_2 nanoparticles results in an estimated retention of Tc of 10^4 years, which is only a fraction of the half-life of Tc (2.1×10^5 years).

Introduction

Technetium (^{99}Tc) is a problematic fission product for nuclear waste disposal due to its long half-life (2.1×10^5 yr), high fission yield (6 %), and the environmental mobility of pertechnetate (TcO_4^-), its stable form in aerobic environments.[1-4] Tc migration may be mitigated by disposal in an anaerobic repository since Tc(IV) is the most stable oxidation state under these conditions and is not highly mobile.[3] Alternatively, Tc may be immobilized in a waste form that is sufficiently durable to prevent the release of Tc until an acceptable fraction has decayed (typically 10 half-lives; however, the period may be shorter or longer depending on the hazard).[5] The current U.S. high-level waste repository, Yucca Mountain, is aerobic.[6] In addition, the majority of the Tc from plutonium production at the Savannah River and Hanford Sites will be disposed of in near-surface, aerobic repositories.[7,8] Disposal of Tc in current and proposed aerobic repositories underscores the interest in durable waste forms for Tc immobilization.

Even under anaerobic conditions, the 3 pM solubility of $TcO_2 \cdot xH_2O$ exceeds the U.S. Environmental Protection Agency maximum contaminant level of 900 pCi/L or 0.5 pM, and naturally occurring ligands can increase Tc(IV) solubility.[9-15] Consequently, durable waste forms are desirable for Tc disposal under anaerobic conditions. The most commonly used waste form,

borosilicate glass, is durable, but loss of volatile Tc species during glass vitrification can decrease Tc retention in the glass.[16-18] Alternatives include synthetic analogs of weathering-resistant, mineral phases, especially Synroc, that accommodate Tc doping.[19-24] Since the effective six coordinate ionic radii of Tc(IV) and Ti(IV), 0.645 Å and 0.604 Å,[25] respectively, are similar, Tc(IV) can replace Ti(IV) in titanium oxides.[19] Titanium dioxide, especially rutile, is highly durable under aerobic conditions, which makes it a particularly attractive matrix for immobilizing Tc.

To date, Tc doped titanium oxides have been prepared by high temperature routes. Mueller and Roy demonstrated that TcO_2 is fully miscible with TiO_2.[19] Notably, Vance and coworkers at ANSTO have doped Tc(IV) into a variety of titanates, as well as TiO_2, by hot isostatic pressing (HIPing).[26,27] Other examples include incorporation of Tc(IV) into magnesium titanate spinel (Mg_2TiO_4) by Khalil and White and gadolinium titanate pyrochlores ($Gd_2Ti_2O_7$) by Hartmann and coworkers.[28-31] While high temperature routes, including vitrification and HIPing, create dense nuclear waste forms, Tc poses challenges. In the case of vitrification (>1000 °C), loss of volatile Tc(VII) species can occur under oxidizing conditions.[22] HIPing involves sealing the precursor inside a sealed canister prior to pressing, which prevents loss of volatile Tc species. However, maintaining Tc in the desired oxidation state during HIPing is challenging. While most Tc is incorporated into the titanate matrix during HIPing, some may be present as pertechnetate or metallic inclusions, which are less resistant to Tc leaching.[26,27]

An approach that has not been extensively explored is doping Tc(IV) into TiO_2 using aqueous chemistry, which may be easier to implement than high temperature routes and can be

compatible with existing waste streams from reprocessing spent nuclear fuel. This approach could improve Tc retention in titanate phases during hot pressing as Tc could be dispersed within the titanate phase prior to heat treatment, reducing the likelihood that Tc would exist as pertechnetate or metal in the final waste form. Aqueous routes produce TiO_2 nanoparticles rather than the dense, low specific surface area materials that are achievable through hot pressing, so the as-prepared Tc-doped TiO_2 material might not be capable of immobilizing Tc without further treatment.

This report describes an aqueous route to Tc-doped TiO_2 starting from TcO_4^- in nitric acid, which is a surrogate for the Tc waste stream from the UREX+ family of separations.[32] The chemistry also applies to the PUREX waste stream, which has a lower nitric acid concentration.[33] The solution was denitrated using formic acid to produce TcO_4^- in a mixture of ~0.1 M HNO_3 and ~0.4 M HCOOH.[34] This denitrated solution was treated with titanium powder and ammonium fluoride yielding Tc-doped TiO_2 (anatase) after 16 hr to 48 hr at reflux. These conditions are similar to the process for removing Zircaloy cladding from used nuclear fuel (Zirflex process).[35] This approach is also similar to the direct oxidation route to TiO_2 nanorods;[36,37] however, the oxidizer used here is residual nitrate rather than hydrogen peroxide. The resulting material was characterized by X-ray diffraction (XRD), X-ray absorption fine structure spectroscopy, and diffuse reflectance visible spectroscopy, which indicate that Tc replaces Ti in the TiO_2 lattice and that Tc is present as Tc(IV) dimers. The release of Tc from the doped TiO_2 into deionized water under aerobic conditions was followed for 8 months.

Experimental

Caution: Tc is β−emitter. All operations were carried out in a laboratory equipped to handle this isotope. All handling of uncontained Tc and all reactions were carried out in a fume hood that was posted as a radioactive contamination area. Required personal protective equipment (PPE) are safety glasses, lab coat, and disposable gloves taped to the lab coat. An additional pair of disposable gloves is required if Tc contamination of the gloves is plausible. PPE and the work were surveyed frequently using a "pancake" Geiger-Mueller (G-M) probe. The entire work area was smeared and counted at the end of each work day. All technetium samples and all other chemicals in the fume hood were disposed as radioactive waste. At the end of the project, the entire inner surface of the fume hood was scrubbed with dilute, aqueous Na_2EDTA to remove Tc from the stainless steel.

General. Deionized (DI) water was obtained from a Milli-Q Gradient A-10 system. Titanium powder (325 mesh, 99.98% Ti) was purchased from Aldrich and ground in a mortar and pestle for 1 minute prior to use. (Note: the syntheses described below failed when using an aqueous slurry of 20 μm Ti powder, possibly due to a thicker surface coating of TiO_2). Other chemicals were ACS grade or better and were used as received. pH was determined using a VWR pH meter with an Orion ROSS pH electrode, which was calibrated daily using pH 4 and pH 7 buffers or pH 7 and pH 10 buffers. Acid concentration was determined by titration with 0.100 M KOH.

Liquid Scintillation Counting (LSC). Solutions (1.8 mL) were centrifuged (5 min, 8500 g) to remove Tc-doped TiO_2. 1 mL of the supernate was removed and centrifuged (5 min, 8500 g). 10 uL of this doubly-centrifuged solution was added to 4 mL of Ecolume. Samples were analyzed

using a Wallac 1414 liquid scintillation counter. Results were not corrected for quenching. Comparison of the spectral quench parameter, SQP(E), to a ^{99}Tc quench curve prepared using nitromethane showed <1% quenching.

Denitration of TcO_4^- in 5 M HNO_3

A 25 mL, three-neck, round bottom flask was equipped with a heating mantle, stir bar, glass stopper, and a reflux condenser capped with a tee connecting it to a bubbler and an argon line. The vessel was purged with argon for 5 minutes through an open neck of the flask. 8.00 mL of 5.18 M NO_3 was added by pipette followed by 70 uL of 0.15 M TcO_4^- in 0.03 M HNO_3 (1.0 mg of Tc). The open neck was closed with a PTFE-faced silicone septum, and the solution was sparged using a stainless steel needle inserted through the septum and into the solution. Sparging was discontinued when the solution reached reflux. Formic acid (2.35 mL) was added to the refluxing HNO_3 solution using a syringe pump (KD Scientific) at 1.5 mL hr^{-1}.[34,38] Following the addition of HCOOH, the pale yellow solution was heated at reflux for 4 hr yielding a colorless solution. The pH of the denitrated solution varied from 0.5 to 1. A control run (no Tc) had a final pH of 1.0 and contained 0.5 M H^+ by titration, which is consistent with 0.1 M HNO_3 and 0.4 M HCOOH.

Treatment of denitrated solution with Ti powder and NH_4F (Sample 1)

The denitrated solution was allowed to cool to room temperature before Ti powder (24 mg) and NH_4F (20 mg) were added while purging with Ar. The solution quickly turned violet then violet-brown. The solution was sparged with Ar while heating it to reflux. The mixture was heated at reflux for 16 hr producing a brown slurry with a colorless solution. The mixture was allowed to

cool to room temperature, distributed among five 2 mL polypropylene (PP) centrifuge tubes, and centrifuged (5 min, 8500 g). The supernate was collected (7.9 mL, pH 1.7) and 10 uL was counted by LSC (15700 dpm, 33% of Tc in solution). The pink-brown solid was collected and washed twice with 1.5 mL water then 1.5 mL acetone.

Treatment of denitrated solution with Ti powder and NH_4F three times (Sample 2)

Sample **2** was prepared analogously to sample **1** except that the mixture was cooled to room temperature and Ti powder (24 mg) and NH_4F (20 mg) were added three times: after denitration, 6 hr after denitration, and 24 hr after denitration. The mixture was allowed to cool to room temperature, distributed among five 2 mL PP centrifuge tubes, and centrifuged (5 min, 8500 g). The supernate was collected (7.9 mL, pH 4.9) and 10 uL was counted by LSC (53 dpm, 0.1 % of Tc in solution). The pink-brown solid was collected and washed twice with 1.5 mL water, then 1.5 mL acetone.

Preparation of 1′ and 2′ for EXAFS measurements.

1′. As described for **1** except that the amounts of TcO_4^-, Ti powder, and NH_4F were doubled. Final pH was 2.6, and 0.7 % of the Tc remained in solution. Sample **1′** is shown in Figure S4.

2′. As described for **2** except that the amounts of TcO_4^-, Ti powder, and NH_4F were doubled. In addition, Ti powder and NH_4F were added 2 times rather than 3 times. Final pH was 2.0, and 0.6 % of the Tc remained in solution. Sample **2′** is shown in Figure S4.

Room temperature leaching experiments. All handling was performed in air using solutions equilibrated with air at room temperature (20 °C). Tc doped TiO_2 was suspended in 10.0 mL DI water by sonication. The slurry was added to 15 mL PP centrifuge tubes, which were placed on a rocking table and rocked at 0.5 Hz to keep the material in suspension. The Tc concentration was measured by LSC. The amount of Tc released into solution was determined from the Tc concentration using the initial volume of water, 10.0 mL. Both the solid and supernate removed for LSC analysis were placed back in their original 15 mL tubes. The initial amount of Tc in the leaching experiments was determined from the Tc retained in the solid (by LSC counting the supernate) minus the amount in the XRD samples (6 % determined by directly counting the XRD samples). Over the course the leaching experiment, 8 months, the initially brown solid turned pink. This pink solid was isolated by distributing it among PP centrifuge tubes, centrifuged (8500 g, 5 min), retaining the supernate to measure the pH and Tc concentration, and washing the solid with 1.5 mL water, then 1.5 mL acetone. The materials isolated after leaching **1** and **2** will be referred to as **1a** and **2a**.

X-ray diffraction (XRD). Tc-doped TiO_2 was suspended in acetone. A portion was drawn into a plastic Pasteur pipette, dropped onto a silicon zero background plate, and allowed to dry. Due to the different densities and particle sizes of TiO_2 and Ti, the relative amounts of Ti and TiO_2 are not quantitative (Ti metal precipitates more rapidly, and the amount of Ti in the diffraction sample varies depending on how long after agitation a sample was drawn into the pipette). Samples were sealed with Kapton film to control contamination. Diffraction patterns were recorded using a Panalytical X′Pert Pro diffractometer with a Co source and a silicon strip detector. Data were summed and analyzed using HiScore Plus software.[39] The diffraction data

were modeled using the crystal structures of titanium metal and anatase. Rietveld refinement using Panalytical High Score Plus was used to determine the lattice parameters and to estimate the size of the crystallites.

X-ray absorption fine structure (XAFS) measurements. Samples **1′** and **2′** were dispersed in water, centrifuged (5 min, 8500 g), and the liquid was discarded to produce a homogeneous pellet. Sample **2**a was washed with 1 mL acetone and dried. It was mixed with boron nitride powder until uniform and pressed into an aluminum holder with Kapton windows. Data were obtained at room temperature at the Tc K-edge on Beamline 11-2 of the Stanford Synchrotron Radiation Lightsource. X-rays were monochromatized using a double-crystal monochromator with Si [220] $\phi = 90$ crystals; the second crystal was detuned by 70% to reduce the harmonic content of the beam. Spectra were recorded in transmission using argon filled ion chambers (**1′** and **2′**) or in fluorescence using a 100 pixel germanium detector (**2a**).

Raw data were averaged and corrected for detector dead time using the program Six Pack. Spectra were analyzed by standard procedures[40] using ifeffit[41] and Artemis/Athena.[42] Theoretical scattering curves were calculated using Feff6[43] based on the structure of brookite (TiO_2) with Tc in the octahedral Tc(IV) site.[44] The EXAFS model was a mixture of TcO_4^- and Tc(IV) in the titanium site of brookite. In each phase, the coordination numbers were fixed (e.g., 4 O for TcO_4^-). The fraction of Tc in the phases was allowed to vary with a sum equal to 1 (e.g., 0.15 Tc in TcO_4^- and 0.85 Tc in brookite). The coordination number in the fit is the fraction of the phase multiplied by the number of scattering atoms (e.g., the 15% of Tc in TcO_4^- has 0.6 O neighbors). The statistical significance of each scattering shell was evaluated using an F-test.[45]

Tc K-edge XANES spectra were fit using the locally written code "fites" and the spectra of TcO_4^-, $TcO_2 \cdot xH_2O$, and $[(H_2EDTA)Tc]_2(\mu\text{-}O)_2$ as the standards. The latter reflects Tc(IV) in a highly distorted octahedral environment, which may be applicable to Tc(IV) adsorbed to the surface of TiO_2. The statistical significance of the contribution of each standard was evaluated using an F-test.[45]

Diffuse reflectance visible spectroscopy. Diffuse reflectance data were collected using an Ocean Optics ST2000 spectrometer with a QR400-7-SR diffuse reflectance probe at 45°. Samples were prepared by pressing PTFE powder in a 0.25 inch by 0.5 inch slot in an 0.1 inch thick aluminum holder. A drop of the sample suspended in acetone was dropped onto the PTFE pellet and allowed to dry. The background was recorded on PTFE without the added sample. The spectra were fit in Excel as sums of pseudo-Voigt peaks.

EPR spectroscopy. A small amount of each sample was drawn into 1.4 mm ID by 1.9 mm OD polyethylene (PE) tubing, which was subsequently heat-sealed at both ends. The sealed tubing was placed into 4 mm quartz tubing, which was filled with He gas and flame sealed. Electron paramagnetic resonance (EPR) spectra were obtained at 2 K with a Varian E-12 spectrometer equipped with liquid helium cryostat, an EIP-547 microwave frequency counter, and a Varian E-500 Gaussmeter calibrated using 2,2-diphenyl-1-picrylhydrazyl (DPPH, g = 2.0036). Spectra were fit using a version of ABVG[46] modified to fit spectra using the downhill simplex method.[47] The code was also modified to use a Pilbrow lineshape, σ_{vi} given in eq 1[48] where g_i is the g-value, β is the Bohr magneton, H is the magnetic field, ν is the microwave frequency, A_i is the

hyperfine coupling constant in cm^{-1}, σ_{Ri} is the residual linewidth, σ_{gi} is the g-strain, σ_{Ai} is the A-strain, and l_i is the direction cosine.

$$\sigma_{vi}^2 = \sum_{i=1}^{3}\left[\sigma_{Ri}^2 l_i^2 + \left(\frac{\beta H g_i}{\upsilon g}\sigma_{gi} + M_I \frac{A_i g_i^2}{A g^2}\sigma_{Ai}\right)^2 l_i^4\right], \text{ where } g^2 = \sum_{i=1}^{3} g_i^2 l_i^2;\ A^2 = \sum_{i=1}^{3} A_i^2 g_i^2 l_i^2$$

(eq 1)

Results

Incorporation of Tc into TiO_2. The primary goal was incorporating Tc into TiO_2 starting from TcO_4^- in HNO_3. In the initial attempts, $Ti(OiPr)_4$ was added to TcO_4^- in 5 M HNO_3 prior to denitration by HCOOH.[34,38] The commercially available titanium alkoxide was used for two reasons. It dissolves readily in 5 M HNO_3, which was anticipated to enhance coprecipitation of Tc(IV) with TiO_2, and isopropanol would react with HNO_3 and decrease the amount of HCOOH required to dentitrate the solution. Although $Ti(OiPr)_4$ dissolved readily in 5 M HNO_3, TcO_4^- largely remained in solution during denitration while TiO_2 (rutile) precipitated as the pH increased. Inadequate Tc reduction and incorporation into TiO_2 is presumably due to the inability of HCOOH, E_0 = 0.2 V, to reduce TcO_4^-, E_0 = 0.74 V, in the presence of nitrate, E_0 = 0.96 V.

To address this redox problem, Ti powder (E_0 = -0.86 V) was used as both the precursor to TiO_2 and a reductant capable of reducing TcO_4^- to Tc(IV). Addition of Ti powder alone to the denitrated solution resulted in no observable reaction and no removal of TcO_4^- from solution, presumably due to the presence of an inert TiO_2 surface layer. To remove this layer, NH_4F was added along with the Ti powder. Treatment of Ti metal with NH_4F has been used previously to prepare TiO_2 nanotubes by direct oxidation and controlled anodization.[36,37,49] In addition,

hydrothermal treatment of Ti metal with NaF has been used to prepare brookite.[50] When both Ti powder and NH_4F were added to the denitrated solution, two thirds of the Tc was removed from solution (sample **1)**. To better remove TcO_4^- from solution, the denitrated solution was treated with Ti/NH_4F three times (sample **2**), which removed 99.9 % of the Tc from solution.

Leaching of Tc from Tc-doped TiO_2

Samples were suspended in 10 mL of deionized (DI) water by sonication, placed in 15 mL centrifuge tubes, continuously rocked to keep the TiO_2 in suspension, and sampled periodically to determine the amount of Tc in solution. As shown in Figure 1, release of Tc is characterized by an initial rapid release of 1 to 3 % of the Tc from the solid followed by a slower release. The release of Tc from **2** appears to decrease from 2 % to 1 % at the beginning of the experiment. The higher initial concentrations of Tc is believed to result from the incomplete removal of Tc-doped TiO_2 nanoparticles by centrifugation of the LSC samples. As the samples aged, agglomeration of the nanoparticles presumably improved the effectiveness of centrifugation resulting in a lower apparent concentration of Tc in solution. The final pH of the solutions were 3.8 and 4.2 for **1** and **2**, respectively. Over the 8 month period that the samples were leached, the color of the samples changed from brown to pink. The pink solids isolated after leaching **1** and **2** will be referred to as **1a** and **2a**, respectively.

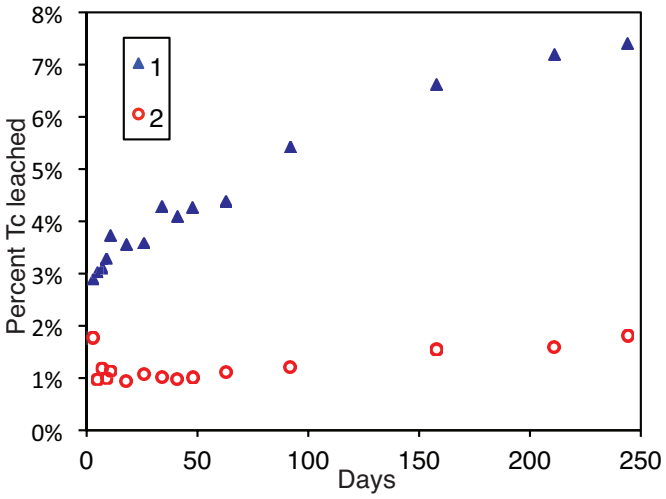

Figure 1. Percent Tc leached from Tc-doped TiO_2 into aerated DI water

X-ray diffraction (XRD). The XRD patterns were recorded before and after leaching to determine which TiO_2 polymorph was formed initially and to determine whether leaching had any significant effect on the lattice parameters or crystallite sizes of the TiO_2 particles (Figure 2 and Table 1). The TiO_2 phase was anatase, and the only other phase observed by XRD was unreacted titanium metal. The crystallite (particle) size for **1** is significantly larger than for **2**, which is likely due to the pH, 1.7, at which **1** was prepared. The low pH increases the amount of dissolved Ti(IV) and presumably facilitates more rapid recrystallization, which produces larger particles by Ostwald ripening. The lattice parameters and crystallite sizes determined before and after leaching were not significantly different.

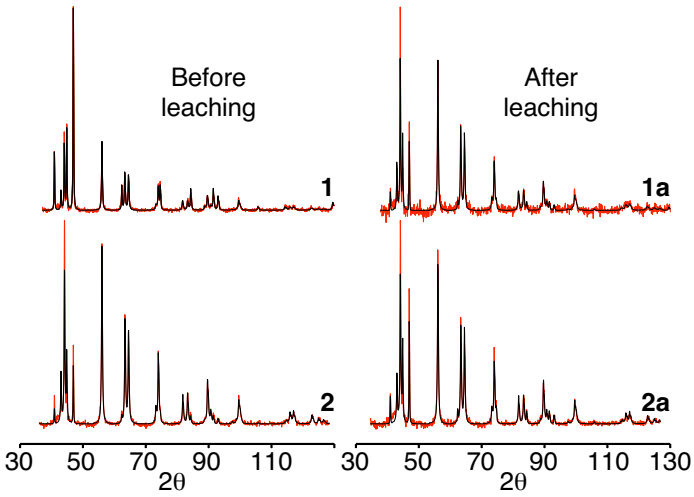

Figure 2: X-ray powder patterns (in red) and Rietveld fits (black) of **1-2** before and after leaching. Data are normalized so that the largest peaks have the same height. Background determined during Rietveld refinement has been subtracted from the diffraction patterns.

Table 1: Diffraction results for Tc-doped TiO_2 before and after leaching

Sample	Phase	a (Å)	c (Å)	Crystallite size (Å)
1 (before)	73% anatase	3.8042(1)	9.5207(3)	1260
	27% Ti metal	2.9505(1)	4.6832(2)	1360
1a (after)	96% anatase	3.8036(2)	9.5198(7)	1110
	4% Ti metal	2.9496(3)	4.6840(9)	559
2 (before)	97% anatase	3.8040(1)	9.5104(4)	550
	3% Ti metal	2.9495(2)	4.6865(8)	700
2a (after)	94% anatase	3.8032(1)	9.5135(4)	570
	6% Ti metal	2.9495(2)	4.6838(4)	790

X-ray Absorption Fine Structure (XAFS) spectroscopy of Tc doped TiO_2

To prepare larger samples for EXAFS spectroscopy, **1′** and **2′** were prepared analogously to **1** and **2** except the amount of Tc, Ti and NH_4F was doubled. In addition, **2′** involves only two additions of Ti powder and NH_4F. The spectrum of **2a** was also recorded. The Tc K-edge EXAFS spectra are shown in Figure 3. The fitting results are provided in Table 2 along with the local structure of Ti in brookite. In these samples, Tc is predominantly present as Tc(IV) as indicated by a Tc-O distance of 2 Å. Some TcO_4^- is present, indicated by the 1.75 Å Tc-O distance. EXAFS fitting estimates that 15 % of the Tc is present as TcO_4^- in all samples. The

amount of TcO_4^- may be more accurately determined by XANES fitting, which shows 8 %, 5 %, and 6 % of the Tc is present as TcO_4^- in **1′**, **2′**, and **2a**, respectively (Table **S1**). The local structure of Tc is similar to that of Ti in brookite with the primary difference that the nearest metal neighbor to Tc is Tc rather than titanium. In addition, the Tc-Tc distance is shorter than the Ti-Ti distance in brookite. These results suggest that Tc is present as octahedral, edge-sharing Tc(IV) pairs rather than isolated Tc(IV) ions. Attempts to fit the data with one or two Ti neighbors rather than Tc produced negative σ^2 values, which supports the assignment of the nearest metal neighbor to Tc. Otherwise, the local environment of Tc in these materials is similar to that of Ti in brookite.

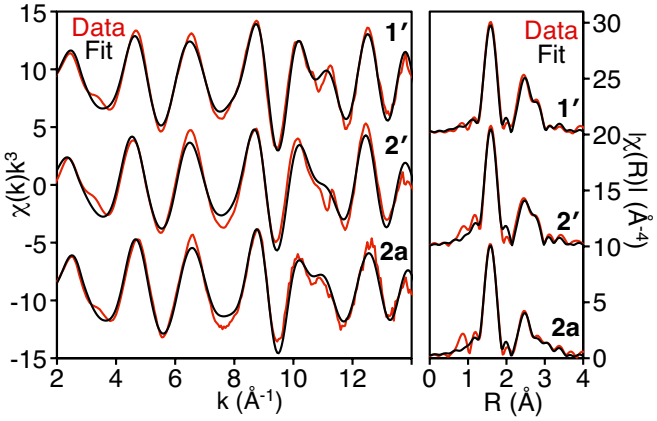

Figure 3. Tc K-edge EXAFS spectra of Tc in TiO_2 (left) and Fourier transforms (right). Data are shown in color and EXAFS fits are shown in black. From top to bottom, spectra are for samples **1′**, **2′**, and **2a**.

Table 2. Local environment of Tc in **1′**, **2′**, and **2** (post leaching) from Tc K-edge EXAFS fitting

Neighbor	# of Neighbors	Distance (Å)	σ^2 (Å^2)	p[a]	Brookite
		Sample **1′**[b]			
O	0.7(1)	1.73(1)	0.001[c]	<0.001	--
O	5.0(2)	2.047(8)	0.0049(5)	<0.001	6 O @ 1.88-2.04
Tc	0.84(3)	2.900(7)	0.0012(5)	<0.001	1 Ti @ 2.965
Ti	1.67(6)	3.22(2)	0.005(2)	0.069	2 Ti @ 3.06
Ti	3.3(1)	3.41(2)	0.009(2)	0.035	4 Ti @ 3.55
O	9.2(3)	4.00(9)	0.02(2)	0.314	11 O @ 3.60-4.09
		Sample **2′**[d]			
O	0.6(1)	1.75(2)	0.001[c]	0.009	--
O	5.1(2)	2.04(1)	0.0041(6)	<0.001	6 O @ 1.88-2.04
Tc	0.85(4)	2.90(2)	0.0022(8)	0.027	1 Ti @ 2.965
Ti	1.71(7)	3.24(5)	0.008(6)	0.425	2 Ti @ 3.06
Ti	3.4(1)	3.44(5)	0.012(6)	0.307	4 Ti @ 3.55
O	9.4(4)	4.0(1)	0.02(2)	0.553	11 @ O 3.4-3.7
		Sample **2** (post leaching)[e]			
O	0.6(1)	1.74(1)	0.001[c]	0.001	--
O	5.1(1)	2.038(7)	0.0049(5)	<0.001	6 O @ 1.88-2.04
Tc	0.85(2)[c]	2.900(8)	0.0023(6)	<0.001	1 Ti @ 2.965
Ti	1.71(5)	3.21(2)	0.004(2)	0.011	2 Ti @ 3.06
Ti	3.4(1)	3.42(2)	0.009(2)	0.002	4 Ti @ 3.55
O	9.4(3)	4.00(8)	0.02(1)	0.112	11 O @ 3.60-4.09

a) Probability that the improvement to the fit by adding the scattering shell is due to error.
b) ΔE=2(2) eV; fit range 2<k<14; 1<R<5; 24.6 data, 13 parameters, r = 0.027.
c) Parameter fixed at the indicated value
d) ΔE=0(2) eV; fit range 2<k<14; 1<R<5; 24.6 data; 13 parameters, r = 0.042.
e) ΔE=3(1) eV; fit range 2<k<14; 1<R<4; 24.6 data; 13 parameters, r =0 .025.

Diffuse Reflectance Visible Spectroscopy

The visible spectra of **1a** and **2a** were measured using diffuse reflectance (Figure 4). The spectra consist of two peaks in the visible on the tail of a much stronger transition in the UV, presumably from TiO_2.[36] The spectra show a major peak at 20050 cm^{-1} and 19830 cm^{-1} and a much weaker peak at 16150 cm^{-1} and 15450 cm^{-1} for **1a** and **2a**, respectively. These peaks are similar to those of molecular complexes containing edge-sharing Tc(IV) octahedra, such as $[(EDTA)Tc]_2(\mu\text{-}O)_2$, which absorb strongly ~20000 cm^{-1} and absorb more weakly at lower energy (16700 cm^{-1} in

$[(EDTA)Tc]_2(\mu\text{-}O)_2))$.[51-54] The spectra suggest the presence of edge-sharing Tc(IV) octahedra, consistent with the EXAFS results.

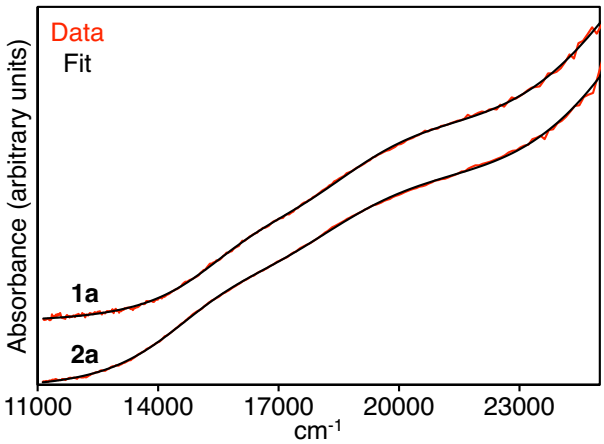

Figure 4. Visible absorption spectra of **1a** and **2a** recorded by diffuse reflectance. Data are shown in color and fits are shown in black.

EPR spectroscopy

The relatively weak EPR spectra of **1a** and **2a** are shown in Figure 5. The Tc(IV) dimers identified by EXAFS are not expected to be EPR active since their molecular analogs are diamagnetic. The EPR spectra are likely due to a minor Tc species. The spectra are almost identical and can be simulated using a nuclear spin of 9/2 and the parameters given in the caption of Figure 5. The EPR spectra indicate that all EPR active Tc ions have similar coordination environments. The g-values and hyperfine coupling constants (A-values) are not particularly similar to any reported for Tc(IV) or Tc(VI).[55-57] The most similar values are those of $TcO_2 \cdot xH_2O$.[58] EPR spectroscopy indicates that some EPR-active Tc species are present in the samples; however, the specific species responsible for the spectrum could not be identified.

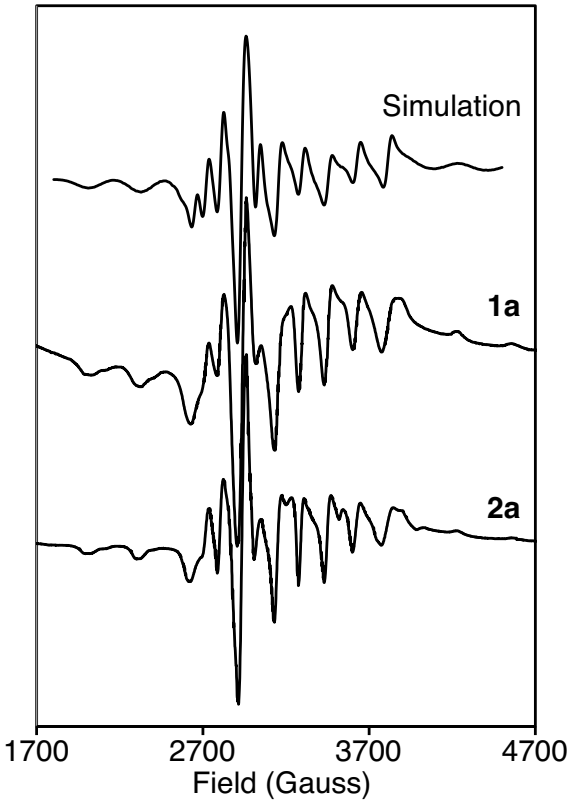

Figure 5. EPR spectra of Tc in TiO_2 after leaching (**1a** and **2a**). EPR spectrum simulated using an effective S′=1/2 spin Hamiltonian with $g_1 = 2.056$, $g_2 = 2.011$, $g_3 = 1.899$, $|A_1| = 7.2\times10^{-3}$ cm^{-1}, $|A_2| = 12\times10^{-3}$ cm^{-1}, $|A_3| = 29\times10^{-3}$ cm^{-1}

Discussion

The main result is that Tc-doped TiO_2 may be readily prepared from TcO_4^- in nitric acid by direct oxidation of Ti powder in the presence NH_4F. The approach is simple although the reaction is slow. Even after 16 hr at reflux, some Ti metal is still present. EXAFS and visible spectroscopy demonstrate that Tc(IV) replaces Ti(IV) on lattice sites and that Tc is largely present as edge-sharing, octahedral Tc(IV) pairs. Replacement of Ti by Tc is as expected since Ti(IV) and Tc(IV) are both tetravalent and have similar effective ionic radii, 0.604 Å and 0.645 Å, respectively.[25] Moreover, Tc doped titanates have been previously prepared by high

temperature routes.[19,27-31,59] Likewise, the predominance of Tc-dimers versus isolated Tc(IV) ions is unsurprising. This structural motif is present in TcO_2,[60,61] is common among Tc(IV) complexes in aqueous solution,[51-54] and was predicted by calculations of Tc(IV) doping into rutile.[62]

The only seemingly unusual result is the apparent mismatch between the long-range structure of the titanium oxide phase determined by XRD, anatase, and the local structure of Tc(IV) determined by EXAFS, which resembles brookite. As noted by Zhang and Banfield, anatase and brookite are polytypes differing only in the stacking arrangement of structurally similar layers of Ti(IV) octahedra.[63] Moreover, twin planes in anatase have the brookite structure.[63] In Tc-doped TiO_2, Tc appears to occupy sites at twin planes of anatase. The preference of Tc for these sites is presumably due to two factors. The average Ti-O distance in anatase and brookite is 1.934 Å and 1.960 Å,[64,65] respectively, so substitution of the Ti site by Tc, which is slightly larger, will cause less distortion in brookite. Likewise, the shortest Ti-Ti distances in anatase and brookite are 3.039 Å, and 2.951 Å,[64,65] so replacing a pair of Ti atoms with a Tc-Tc dimer with a short Tc-Tc distance will result in less distortion in the brookite structure.

A more relevant issue with respect to nuclear waste is Tc retention by **1** and **2**. The leaching data in Figure 1 can be used to address two related factors – the effectiveness of TiO_2 as a matrix for retaining Tc and how well these specific samples retain Tc. The effectiveness of the TiO_2 matrix is given by the normalized release rate (LR), which as calculated using eq 2 where m_{Tc} is the mass of Tc lost, ρ is the density of TiO_2, D is the particle size (crystallite diameter from XRD),

m is the mass of the sample, f_{Tc} is the mass fraction of Tc in the solid, and t is the time in days (244) (the values of these parameters are collected in Table S2).[66]

$$LR(Tc) = \frac{m_{Tc} \cdot \rho \cdot D}{6m \cdot f_{Tc} \cdot t} \qquad (2)$$

The normalized release rates for **1** and **2** are 4×10^{-5} g m^{-2} d^{-1} and 3×10^{-6} g m^{-2} d^{-1}, respectively, at 20 °C. For comparison, the normalized rate of titanium leaching from Synroc C is 2×10^{-5} g m^{-2} d^{-1} at 95 °C,[20] which corresponds to 2×10^{-6} g m^{-2} d^{-1} at 21 °C using a typical activation energy for Synroc leaching (30 kJ mol^{-1}).[66] The similarity of the Ti leach rate in Synroc C to the Tc leach rates from **1** and especially **2** are consistent with the hypothesis that Tc is doped into TiO_2 as indicated by EXAFS spectroscopy since Tc is being released from **1** and **2** at rates similar to Ti release from a titanate matrix. In addition, the normalized leach rates indicate that TiO_2 is a highly effective matrix for immobilizing Tc. However, normalized leach rates do not indicate whether **1** and **2** themselves are effective waste forms.

To evaluate how well **1** and **2** would retain Tc, two empirical models were used: the dissolving particle model and diffusion model.[67] In the dissolving particle model, the outer layer of the TiO_2 particle dissolves, and any Tc in this layer goes into solution.[67] In the diffusion model, the TiO_2 particles do not dissolve, and Tc slowly diffuses out of the TiO_2 particles.[67] The time needed for all of the Tc to enter the solution, τ, is given by eq (3) and (4) for the dissolving particle and diffusion models, respectively, where m_{fast} is a variable corresponding to the rapid loss of Tc at the beginning of the experiment.[67] Tc leaching was modeled from day 25 through day 250. The analysis begins at day 25 rather than day zero to allow the concentration of dissolved Ti to approach equilibrium. Results are shown in Figure 6. Using the dissolving particle model, Tc would be fully leached from **1** and **2** after 23 and 110 yr, respectively. In the diffusion model, Tc

would be fully leached from **1** and **2** after 560 and 12000 yr, respectively. Even under this optimistic scenario, all Tc is lost within a fraction of its half-life.

$$\frac{t}{\tau} = 1 - (1 - m_{Tc} - m_{fast})^{2/3} \qquad (3) \text{ dissolving particle}$$

$$\frac{t}{\tau} = 1 - 3(1 - m_{Tc} - m_{fast})^{2/3} + 2(1 - m_{Tc} - m_{fast}) \qquad (4) \text{ diffusion}$$

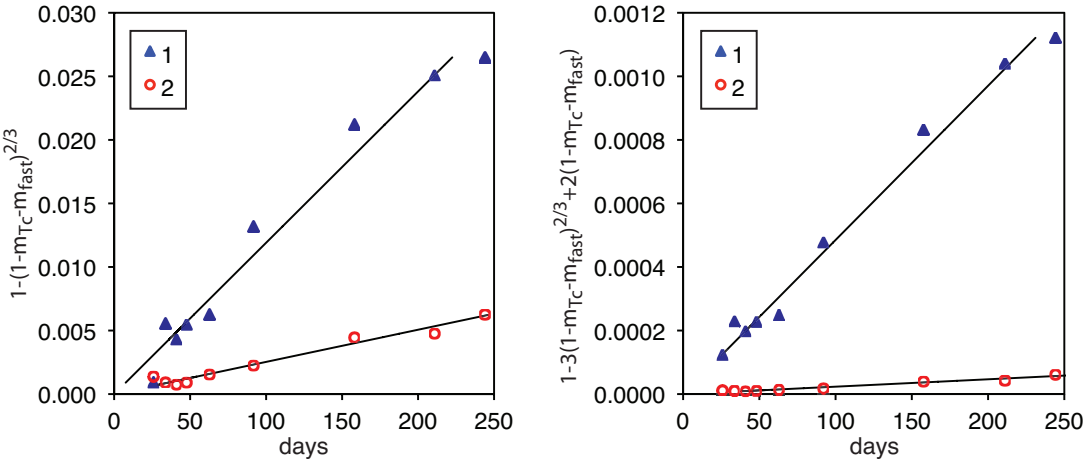

Figure 6. Loss of Tc from Tc-doped TiO_2 modeled using a dissolving particle model (left) and a diffusion model (right). The lines indicate the fit to the data by eq 3 and 4, respectively.

Conclusion

Starting from pertechnetate in nitric acid, technetium may be incorporated into titanium dioxide by chemical denitration using formic acid followed by treatment of the solution with titanium powder and ammonium fluoride. Titanium powder functions as both the reducing agent to reduce TcO_4^- to Tc(IV) and as the precursor to TiO_2. The reaction produces Tc-doped anatase nanoparticles with crystallite diameters of 60 nm to 120 nm. Technetium is incorporated into TiO_2 as edge-sharing Tc(IV) dimers replacing analogous Ti(IV) dimers. From leaching data,

titanium dioxide is an excellent matrix for immobilizing Tc as indicated by the low normalized release rate. However,, **1** and **2** are not effective waste forms due to their small particle sizes and associated high specific surface areas. Immobilizing **1** or **2** in a cementitious matrix would likely result in faster release of Tc due to the higher solubility of Ti(IV) in alkaline pore water. On the other hand, if these materials were consolidated into a dense waste form (e.g., by hot pressing or pressing and sintering), the resulting Tc doped TiO_2 would likely be an effective waste form as indicated by its low normalized release rate (LR_{Tc}). Moreover, use of Tc-doped TiO_2 prepared by aqueous routes as the precursor for waste forms prepared by high temperature routes may improve final hot-pressed waste form since technetium is initially in the desired oxidation state and is dispersed in TiO_2. As a result, Tc may be less likely to end up as pertechnetate or metal inclusions in the final waste form.

Supporting Information. Experimental descriptions for treatment of TcO_4^- in HNO_3 with Ti(O-i-Pr)$_4$ and with Ti powder alone, XANES spectra and fitting results, and photographs of samples **1′**and **2′** are given in the SI.

The Supporting Information is available free of charge on the ACS Publications website.

Acknowledgement

This work was supported by the U.S. Department of Energy (DOE), Office of Science, Basic Energy Sciences, Chemical Sciences, Biosciences, and Geosciences Division (CSGB), Heavy Element Chemistry Program and was performed at Lawrence Berkeley National Laboratory under contract No. DE-AC02-05CH11231. Tc K-edge XAFS spectra were obtained at the Stanford Synchrotron Radiation Lightsource (SSRL), SLAC National Accelerator Laboratory, which is supported by the U.S. Department of Energy, Office of Science, Office of Basic Energy Sciences under Contract No. DE-AC02-76SF00515. Travel to SSRL (SAS) was supported by the DOE Waste Treatment and Immobilization Plant Project of the Office of River Protection. PNNL is operated for the DOE by Battelle Memorial Institute under Contract DEAC05-76RL01830.

References

(1) Icenhower, J. P.; Qafoku, N. P.; Zachara, J. M.; Martin, W. J. The Biogeochemistry of Technetium: a Review of the Behavior of an Artificial Element in the Natural Environment. *Am. J. Sci.* **2010**, *310*, 721-752.
(2) Pilkington, N. J. The Solubility of Technetium in the Near-Field Environment of a Radioactive-Waste Repository. *J. Less Common Met.* **1990**, *161*, 203-212.
(3) Kunze, S.; Neck, V.; Gompper, K.; Fanghanel, T. Studies on the Immobilization of Technetium under Near Field Geochemical Conditions. *Radiochim. Acta* **1996**, *74*, 159-163.
(4) Ishii, T.; Sakuragi, T. Technetium in the Environment. *Radioisotopes* **2006**, *55*, 485-494.
(5) Hebel, L. C.; Christensen, E. L.; Donath, F. E.; Falconer, W. E.; Lidofsky, L. J.; Moniz, E. J.; Moss, T. H.; Pigford, R. L.; Pigford, T. H.; Rochlin, G. I.; Silsbee, R. H.; M.E., W.; Frauenfelder, H.; Cairns, T. L.; Panofsky, W. K. H.; Simmons, M. G. Report to the American Physical Society by the Study Group on Nuclear Fuel Cycles and Waste Management. *Rev. Mod. Phys.* **1978**, *50*, S1-S185.
(6) *Yucca Mountain Repository License Application*, DOE/RW-0573, Rev. 0, U.S. Department of Energy, 2008.
(7) Mann, F. M.; Puigh, R. J.; Finfrock, S. H.; Khaleel, R.; Wood, M. I. *Integrated Disposal Facility Risk Assessment*, RPP-15834, CH2M Hill Hanford Group, Inc., 2003.

(8) *Performance Assessment for the Saltstone Disposal Facility at the Savannah River Site*, SRR-CWDA-2009-00017, SRR Closure & Waste Disposal Authority, 2009.
(9) *EPA facts about Technetium-99*, U.S. Environmental Protection Agency, 2014.
(10) Liu, D. J.; Yao, J.; Wang, B.; Bruggeman, C.; Maes, N. Solubility Study of Tc(IV) in a Granitic Water. *Radiochim. Acta* **2007**, *95*, 523-528.
(11) Hess, N. J.; Xia, Y. X.; Rai, D.; Conradson, S. D. Thermodynamic Model for the Solubility of $TcO_2 \cdot xH_2O$(am) in the Aqueous Tc(IV)-Na^+-Cl^--H^+-OH^--H_2O Aystem. *J. Solution Chem.* **2004**, *33*, 199-226.
(12) Gu, B. H.; Dong, W. M.; Liang, L. Y.; Wall, N. A. Dissolution of Technetium(IV) Oxide by Natural and Synthetic Organic Ligands Under both Reducing and Oxidizing Conditions. *Environ. Sci. Technol.* **2011**, *45*, 4771-4777.
(13) Boggs, M. A.; Minton, T.; Dong, W. M.; Lomasney, S.; Islam, M. R.; Gu, B. H.; Wall, N. A. Interactions of Tc(IV) with Humic Substances. *Environ. Sci. Technol.* **2011**, *45*, 2718-2724.
(14) Sekine, T.; Watanabe, A.; Yoshihara, K.; Kim, J. I. Complexation of Technetium with Humic Acid. *Radiochim. Acta* **1993**, *63*, 87-90.
(15) Yalcintas, E.; Gaona, X.; Altmaier, M.; Dardenne, K.; Polly, R.; Geckeis, H. Thermodynamic Description of Tc(IV) Solubility and Hydrolysis in Dilute to Concentrated NaCl, $MgCl_2$ and $CaCl_2$ Solutions. *Dalton Trans.* **2016**, *45*, 8916-8936.
(16) Migge, H. Simultaneous Evaporation of Cs and Tc during Vitrification-a Thermochemical Approach. *Mater. Res. Soc. Symp. Proc.* **1990**, *176*, 411-417.
(17) Lammertz, H.; Merz, E.; Halaszovich, S. Technetium Volatilization During HLW Vitrification. *Mater. Res. Soc. Symp. Proc.* **1985**, *44*, 823-829.
(18) Bibler, N. E.; Fellinger, T. L.; Marra, S. L.; O'Driscoll, R. J.; Ray, J. W.; Boyce, W. T. Tc-99 and Cs-137 Volatility from the DWPF Production Melter During Vitrification of the First Macrobatch of HLW Sludge at the Savannah River Site. *Mater. Res. Soc. Symp. Proc.* **2000**, *608*, 697-702.
(19) Muller, O.; White, W. B.; Roy, R. Crystal Chemistry of Some Technetium-Containing Oxides. *J. Inorg. Nucl. Chem.* **1964**, *26*, 2075-2086.
(20) Ringwood, A. E. Disposal of High-Level Nuclear Waste: a Geological Perspective. *Mineral. Mag.* **1985**, *49*, 159-176.
(21) Ringwood, A. E.; Kesson, S. E.; Ware, N. G.; Hibberson, W.; Major, A. Immobilization of High-Level Nuclear Reactor Wastes in Synroc. *Nature* **1979**, *278*, 219-223.
(22) Luksic, S. A.; Riley, B. J.; Schweiger, M.; Hrma, P. Incorporating Technetium in Minerals and Other Solids: A Review. *J. Nucl. Mat.* **2015**, *466*, 526-538.
(23) Ackerman, M.; Kim, E.; Weck, P. F.; Chernesky, W.; Czerwinski, K. R. Technetium Incorporation in Scheelite: Insights from First-Principles. *Dalton Trans.* **2016**, *45*, 18171-18176.
(24) Weck, P. F.; Kim, E.; Poineau, F.; Rodriguez, E. E.; Sattelberger, A. P.; Czerwinski, K. R. Structural and Electronic Trends in Rare-Earth Technetate Pyrochlores. *Dalton Trans.* **2010**, *39*, 7207-7210.
(25) Shannon, R. D. Revised Effective Ionic-Radii and Systematic Studies of Interatomic Distances in Halides and Chalcogenides. *Acta Cryst. A* **1976**, *32*, 751-767.
(26) Vance, E. R.; Carter, M. L.; Day, R. A.; Begg, B. D.; Hart, K. P.; Jostsons, A. Synroc and Synroc-Glass Composite Waste Forms for Hanford HLW Immobilization. *Proceedings of the International Topical Meeting on Nuclear and Hazardous Waste Management. Spectrum '96* **1996**, 2027-2031.

(27) Hart, K. P.; Vance, E. R.; Day, R. A.; Begg, B. D.; Angel, P. J.; Jostsons, A. Immobilization of Separated Tc and Cs/Sr in Synroc. *Mater. Res. Soc. Symp. Proc.* **1996**, *412*, 281-287.
(28) Khalil, M. Y.; White, W. B. Magnesium Titanate Spinel - a Ceramic Phase for Immobilization of Tc-99 from Radioactive Wastes. *J. Am. Ceram. Soc.* **1983**, *66*, C197-C198.
(29) Khalil, M. Y.; White, W. B. Dissolution of Technetium from Nuclear Waste Forms. *Mater. Res. Soc. Symp. Proc.* **1984**, *26*, 655-662.
(30) Hartmann, T.; Alaniz, A. J.; Antonio, D. J. Fabrication and Properties of Technetium-Bearing Pyrochlores and Perovskites as Potential Waste Forms. *Procedia Chem.* **2012**, *7*, 622-628.
(31) Hartmann, T.; Alaniz-Ortez, A. J. Fabrication and Chemical Durability of Ceramic Technetium-based Pyrochlores and Perovskites as Potential Waste Forms *Adv. Sci. Technol.* **2014**, *94*, 85-92.
(32) Vandegrift, G. F.; Regalbuto, M. C.; Aase, S.; Bakel, A.; Battisti, T. J.; Bowers, D.; Byrnes, J. P.; Clark, M. A.; Cummings, D. G.; Emery, J. W.; Falkenberg, J. R.; Gelis, A. V.; Pereira, C.; Hafenrichter, L.; Tsai, Y.; Quigley, K. J.; Van der Pol, M. H. Designing and Demonstration of the UREX+ Process Using Spent Nuclear Fuel. *ATALANTE 2004: Advances for Future Nuclear Fuel Cycles.* Nimes, France, 2004.
(33) McKibben, J. M. Chemistry of the PUREX Process. *Radiochim. Acta* **1984**, *36*, 3-15.
(34) Bradley, R. F.; Goodlett, C. B. *Denitration of Nitric Acid Solution by Formic Acid*, DP-1299, Savannah River Laboratory, 1972.
(35) Swanson, J. L. *The Zirflex Process*, A/CONF.15/P/2429, Hanford Atomic Products Operation, 1958.
(36) Chen, X.; Mao, S. S. Titanium Dioxide Nanomaterials: Synthesis, Properties, Modifications, and Applications. *Chem. Rev.* **2007**, *107*, 2891-2959.
(37) Wu, J.-M.; Hayakawa, S.; Tsuru, K.; Osaka, A. Porous Titania Films Prepared from Interactions of Titanium with Hydrogen Peroxide Solution. *Scripta Mater.* **2002**, *46*, 101-106.
(38) Hwang, D. S.; Lee, E. H.; Kim, K. W.; Lee, K. I.; Park, J. H.; Yoo, J. H.; Park, S. J. Denitration of Simulated High-Level Liquid Waste by Formic Acid. *J. Ind. Eng. Chem.* **1999**, *5*, 45-51.
(39) Degen, T.; Sadki, M.; Bron, E.; König, U.; Nénert, G. The HighScore Suite. *Powder Diffr.* **2014**, *29*, S13-S18.
(40) Koningsberger, D. C.; Prins, R. *X-Ray Absorption: Principles, Applications, Techniques of EXAFS, SEXAFS, and XANES*; John Wiley & Sons: New York, 1988.
(41) Newville, M. IFEFFIT: Interactive XAFS Analysis and FEFF Fitting. *J. Synchrotron Rad.* **2001**, *8*, 322-324.
(42) Ravel, B. ATHENA and ARTEMIS Interactive Graphical Data Analysis using IFEFFIT. *Phys. Scripta* **2005**, *T115*, 1007-1010.
(43) Mustre de Leon, J.; Rehr, J. J.; Zabinsky, S. I.; Albers, R. C. Ab initio Curved-Wave X-ray-Absorption Fine Structure. *Phys. Rev. B* **1991**, *44*, 4146-4156.
(44) Bosi, F.; Halenius, U.; Skogby, H. Crystal Chemistry of the Magnetite-Ulvospinel Series. *Am. Mineral.* **2009**, *94*, 181-189.
(45) Downward, L.; Booth, C. H.; Lukens, W. W.; Bridges, F. A Variation of the F-test for Determining Statistical Relevance of Particular Parameters in EXAFS Fits. *AIP Conf. Proc.* **2007**, *882*, 129.

(46) Daul, C.; Schlapfer, C. W.; Mohos, B.; Ammeter, J.; Gamp, E. Simulation of Electron Paramagnetic Resonance of Randomly Oriented Samples. *Comput. Phys. Commun.* **1981**, *21*, 385-395.
(47) Press, W. H.; Teukolsky, S. A.; Vetterling, W. T.; Flannery, B. P. *Numerical Recipes in Fortran 77 The Art of Scientific Computing Second Edition*; Cambridge University Press: Cambridge, 1992.
(48) Pilbrow, J. R. *Transition Ion Paramagnetic Resonance*; Oxford University Press: Oxford, 1990.
(49) Macák, J. M.; Tsuchiya, H.; Chmuki, P. High-Aspect-Ratio TiO_2 Nanotubes by Anodization of Titanium. *Angew. Chem. Int. Ed.* **2005**, *44*, 2100-2102.
(50) Oota, T.; Yamai, I.; Saito, H. Brookite Formation by the Oxidation of Titanium Metal under Hydrothermal Conditions. *J. Ceram. Soc. Jpn.* **1979**, *87*, 375-382.
(51) Linder, K. E.; Dewan, J. C.; Davison, A. Technetium bis(μ-oxo) Dimers of 1,4,7-Triazacyclononane-N,N',N''-triacetate (TCTA). Synthesis and Characterization of $[(TCTA)Tc(\mu\text{-}O)_2Tc(TCTA)]^{n-}$ (n = 2,3) and the Crystal Structure of Ba_2 $[(TCTA)Tc(\mu\text{-}O)_2Tc(TcTA)](ClO_4)\bullet 9H_2O$. *Inorg. Chem.* **1989**, *28*, 3820-3825.
(52) Burgi, H. B.; Anderegg, G.; Bauenstein, P. Preparation, Characterization, and Crystal, Molecular, and Electronic Structure of $(H_2EDTA)^{99}Tc^{IV}(\mu\text{-}O)_2{}^{99}Tc^{IV}(H_2EDTA)\bullet 5H_2O$. A 2.33 Å Tc-Tc Distance Which May Represent a $\sigma^2\pi^2\delta^{*2}$ Bond. *Inorg. Chem.* **1981**, *20*, 3829-3834.
(53) Anderegg, G.; Muller, E.; Zollinger, K. Preparation, Characterization, Crystal and Molecular Structure of $Na_2[N(CH_2COO)_3{}^{99}Tc(IV)(\mu\text{-}O)_2{}^{99}Tc(IV)N(CH_2COO)_3]\bullet 6H_2O$. *Helv. Chim. Acta* **1983**, *66*, 1593-1598.
(54) Alberto, R.; Anderegg, G. Synthesis and X-ray Structure of New Tc(IV) Oxalato Complex: $K_4[C_2O_4)_2Tc(\mu\text{-}O)_2Tc(C_2O_4)_2]\bullet 3H_2O$). *Inorg. Chim. Acta* **1990**, *178*, 125-130.
(55) Abram, U.; Kirmse, R. EPR Spectroscopy in the Analytical Chemistry of Technetium Complexes. *J. Radioanal. Nucl. Chem.* **1988**, *122*, 311-319.
(56) Kirmse, R.; Abram, U. EPR on Technetium Complexes - a Review. *Isotopenpraxis* **1990**, *26*, 151-159.
(57) Pieper, H. H.; Schwochau, K. Hyperfine and Superhyperfine EPR Spectra of Tc(IV) and Re(IV) in Tin Dioxide Single Crystals. *J. Chem. Phys.* **1975**, *63*, 4716-4722.
(58) Lukens, W. W.; Bucher, J. J.; Edelstein, N. M.; Shuh, D. K. Products of Pertechnetate Radiolysis in Highly Alkaline Solution: Structure of $TcO_2\bullet xH_2O$. *Environ. Sci. Technol.* **2002**, *36*, 1124-1129.
(59) Carter, M. L.; Stewart, M. W. A.; Vance, E. R.; Begg, B. D.; Moricca, S.; Tripp, J. *HIPed Tailored Ceramic Waste Forms for the Immobilization of Cs, Sr, and Tc*, INL/CON-07-12875, 2007.
(60) Reynolds, E.; Zhang, Z.; Avdeev, M.; Thorogood, G. J.; Poineau, F.; Czerwinski, K. R.; Kimpton, J. A.; Kennedy, B. J. Thermal Expansion Behavior in TcO_2. Toward Breaking the Tc−Tc Bond. *Inorg. Chem.* **2017**, *56*, 9219-9224.
(61) Rodriguez, E. E.; Poineau, F.; Llobet, A.; Sattelberger, A. P.; Bhattacharjee, J.; Waghmare, U. V.; Hartmann, T.; Cheetham, A. K. Structural Studies of TcO_2 by Neutron Powder Diffraction and First Principles Calculations. *J. Am. Chem. Soc.* **2007**, *129*, 10244-10248.
(62) Kuo, E. Y.; Qin, M. J.; Thorogood, G. J.; Whittle, K. R.; Lumpkin, G. R.; Middleburgh, S. C. Technetium and Ruthenium Incorporation into Rutile TiO_2. *J. Nucl. Mat.* **2013**, *441*, 380-389.

(63) Zhang, H.; Banfield, J. F. Structural Characteristics and Mechanical and Thermodynamic Properties of Nanocrystalline TiO_2. *Chem. Rev.* **2014**, *114*, 9613-9644.
(64) Meagher, E. P.; Lager, G. A. Polyhedral Thermal Expansion in the TiO_2 Polymorphs: Refinement of the Crystal Structures of Rutile and Brookite at High Temperature. *Can. Miner.* **1979**, *17*, 77-85.
(65) Horn, M.; Schwerdtfeger, C. F.; Meagher, E. P. Refinement of the Structure of Anatase at Several Temperatures. *Z. Kristallogr.* **1972**, *136*.
(66) Campbell, J.; Hoenig, C.; Bazan, F.; Ryerson, F.; Guinan, M.; Van Konynenburg, R.; Rozsa, R. *Properties of SYNROC-D Nuclear Waste Form: A State-of-the-Art Review*, UCRL-53240, Lawrence Livermore National Laboratory, 1982.
(67) Levenspiel, P. *Chemical Reaction Engineering, Third Edition*; John Wiley & Sons: New York, 1999.

TOC Figure: